

Comparison of Structural Behavior of Nanocrystals in Randomly Packed Films and Long-Range Ordered Superlattices by Time-Resolved Small Angle X-ray Scattering

Byeongdu Lee,[†] Paul Podsiadlo,[‡] Sara Rupich,[§] Dmitri V. Talapin,^{‡,§} Tijana Rajh,[‡] and Elena V. Shevchenko^{*,‡}

Advanced Photon Source, Argonne National Laboratory, Argonne, Illinois 60439, Center for Nanoscale Materials, Argonne National Laboratory, Argonne, Illinois 60439, and University of Chicago, Chicago, Illinois 60637

Received August 15, 2009; E-mail: eshevchenko@anl.gov

The nanocrystal (NC) solids attract a lot of attention because of their promise for a variety of applications such as solar cells, light emitting devices, magneto-recording systems, and field effect transistors.¹ The spontaneous self-assembly of objects starting from atoms through macromolecules (NCs, viruses, polymers) to relatively bulk microspheres (opals, etc.) is an intriguing and universal phenomenon in nature. The ability of NCs to form periodic structures by self-assembly is an attractive way to obtain functional devices due to its simplicity. However, the precise control over self-assembly is still a challenging issue. Nowadays, highly organized two- (2D) and three-dimensional (3D) structures can be obtained from colloidal solutions by a Langmuir–Blodgett technique,² slow solvent evaporation,³ spin-casting,^{3b} or slow destabilization of a colloidal solution by adding nonsolvent.⁴ The 3D periodic structures can be obtained as extended films^{3a} or as faceted 3D colloidal crystals (CCs) similar to atomic crystals.^{3a,5} To date, monodisperse NCs were found to form periodic structures with face-centered cubic (*fcc*), hexagonally closed packed (*hcp*), body centered cubic (*bcc*), and simple hexagonal (*shp*) organization.^{3a,6} The interparticle spacing in superlattices (SLs) is determined by the length of capping ligands and by the type of SL. Interparticle spacing is a crucial parameter that dramatically affects electronic^{1d,7} and optical properties of NC solids.⁸ Postpreparative surface modification of NCs is a general approach to tune the interparticle spacing. It typically involves preliminary removal of the initial organic molecules followed by subsequent addition of desired molecules. New surface ligands not only change the interparticle spacing but also affect the self-assembly⁵ as well as electronic^{1d} and optical⁸ properties of NCs. Therefore, for any comparative studies of coupling effects in NC solids, it is important to have identical surface chemistry.

Theoretical calculations and simulations of hard sphere colloids predict that the dense *fcc* structure should be slightly more stable as compared to the dense *hcp* structure.⁹ Experimentally, an *fcc* SL seems to be the most common case for both 3D periodic films (PFs) and CCs, especially in the case of SLs built from hard noninteracting spheres.¹⁰

In highly organized SLs a better matching of energy levels of individual particles can be achieved and, as a result, more efficient carrier transport can be realized.¹¹ However, to date there is no clear understanding what the difference between 3D PFs and CCs is in terms of their lattice structure and interparticle spacing and how different the behavior of highly organized SLs from their randomly packed analogues is. Even though it is widely accepted

that interparticle spacing is determined by the length of surface molecules, very little is known about their arrangement at the surface of NCs and their spatial structure within the NC solid.

In our work we evaluated the difference between randomly packed NCs (disordered films, DFs), PFs, and CCs using the time-resolved small-angle X-ray scattering (SAXS) technique as well as estimated the possibility of manipulation of interparticle spacing by thermal treatment. Time-resolved SAXS is a proven technique to study *in situ* dynamics of SL self-assembly and SL transformation as well as to monitor the nucleation and growth of individual NCs.¹² In previous studies the focus of the research was made mostly on the self-assembly of gold and silver NCs, known to be very unstable against sintering, sometimes even at room temperature during storage.¹³

All three classes of NC solids (DFs, PFs, and CCs) discussed below were made from 70 Å large PbS NCs stabilized with oleic acid. PbS NCs were synthesized according to the protocol described in ref 14 and redispersed in toluene. DFs were obtained by rapid addition of an equal amount of nonsolvent (*i*-PrOH) to toluene solution of PbS NCs and vigorous shaking, a procedure similar to one used for size fractionalization. The precipitate was then deposited on a Si substrate and dried under ambient conditions. PFs were deposited on a Si substrate by drop casting. Different solvent mixtures (toluene, toluene–chloroform, and toluene–tetrachloroethylene) were used to prepare PFs at different evaporation rates. CCs with the average size ranging from 10 to 200 μm were grown by slow destabilization of toluene solution with an equal amount of *i*-PrOH.^{4a} Time-resolved SAXS experiments were run under nitrogen to avoid any oxidation.

CCs formed from the same PbS NCs on different areas of the same Si substrate as well as at different Si substrates exhibited a highly reproducible d_{111} -spacing. Also the SAXS data acquired for different sets of CCs were almost identical after normalization of their intensities indicating the same degree of ordering in CCs. The structure of CCs is well-resolved from SAXS data and can be assigned to the *fcc* lattice (Figure 1). PFs have also possessed a high degree of *fcc* ordering, while demonstrating consistently larger d_{111} -spacing as compared with CCs (Figure 1a). Previously, it was assumed that PFs represented true relaxed structures.^{13b} In our experiments we noticed that, even though the position of d_{111} -spacing was nearly constant for a number of PFs, they revealed different broadening of the SAXS peaks from sample to sample that can be associated with different sizes of crystalline domains in such samples, as well as intermixing of *fcc*, *hcp*, and disordered phases. The position of d_{111} -spacing in PFs is close to the position of d -spacing of DFs. These observations can indicate that capping molecules are less tightly packed within the DFs and PFs as compared to CCs. Real-time annealing experiments (Figures 1e–g,

[†] Advanced Photon Source, Argonne National Laboratory.

[‡] Center for Nanoscale Materials, Argonne National Laboratory.

[§] University of Chicago.

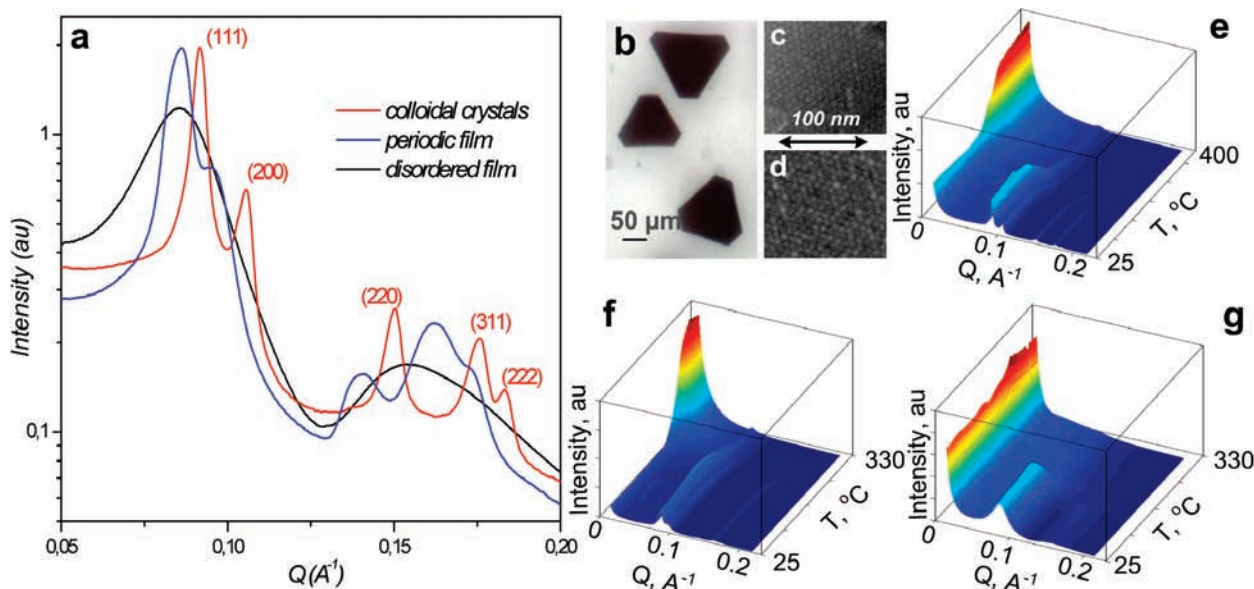


Figure 1. (a) SAXS data obtained for the PbS nanocrystal solids: disordered films (DFs); periodic films (PFs) and colloidal crystals (CCs) at room temperature; (b) optical overview of PbS CCs crystals; (c,d) HRSEM images acquired from the as-prepared CCs and CCs treated at 180 °C for 2 h; (e–g) 3D plots of SAXS data taken during the annealing (10 °C/min) of the CCs, PFs, and DFs, respectively.

2a) demonstrated for all samples showed some minor initial lattice expansion during heating followed by lattice contraction. In the case of DFs and CCs, “lattice” contraction occurred at ~ 182 °C, while, in the PFs, shrinkage of the d_{111} -spacing has been observed after ~ 197 °C. Further annealing led to appearance of gradually developing intensity at a Q lower than 0.0456 \AA^{-1} (Figures 1e–g, S1–S4) that we assigned to the scattering signal from nanosized aggregates that seem to be formed prior to complete collapse of the periodic lattice during partial sintering. The size of aggregates formed during the heating runs can be estimated from SAXS data and is ~ 2 – 3 times that of PbS NCs. In agreement to our observation, probing of coalescence of 2D arrays of PbSe NCs,¹⁵ a system similar to PbS NCs, by *in situ* TEM also revealed that NCs tended to form, first, polyanocrystals that later fused into multidot single crystals. To learn the origin of lattice contraction, we plotted the ratio of intensities of scattered X-rays by aggregates and plane corresponding to the d_{111} -spacing of the *fcc* lattice ($I(q_{\text{agr}})/I(q_{111})$) versus temperature (Figure 2b). No sintering was observed up to ~ 182 °C for DFs. PFs and CCs did not show any sintering

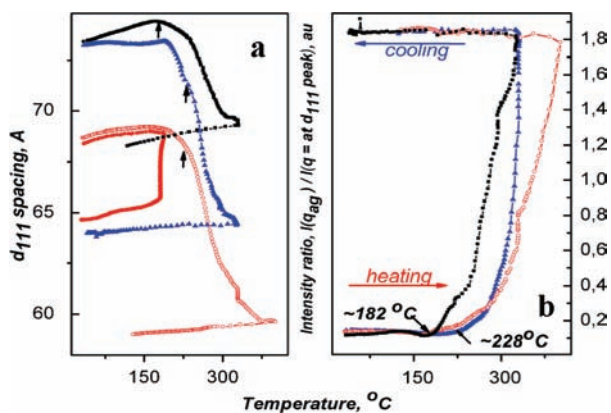


Figure 2. (a) The d_{111} -temperature plot and (b) intensity ratio ($I(q_{<0.0456})/I(q_{111})$)-temperature plots for three types of PbS solids: CCs (filled and empty red circles correspond to different annealing regimes), PFs (blue triangles), and DFs (black squares). Arrows in (a) point to the temperature of sintering onset of PbS NCs.

up to ~ 230 °C. The coincidence of the sintering temperature of DFs and temperature at which their “lattice” contractions occur indicates that “lattice” contraction is accompanied by sintering of individual PbS NCs. Both PFs and CCs have at least an ~ 30 °C window in which individual NCs are stable against sintering and their periodic structure undergoes isotropic contraction. Thermogravimetric analysis (TGA) on these three types of samples has shown a higher concentration of organic molecules in PFs ($\sim 21\%$) as compared to both DFs ($\sim 13\%$) and CCs ($\sim 15\%$) (Figure S5). The surface of PbS NCs is passivated with oleic acid. Assuming that oleic acid is $\sim 4.4 \text{ \AA}$ in width¹⁶ and full coverage of the surface of NCs with oleic acid, we have to expect that $\sim 40 \text{ wt } \%$ should belong to oleic acid. However, the surface of PbS NCs is Pb and S terminated. Oleic acid has been found to passivate only Pb sites, and no indication of OA/S bonding has been observed.¹⁷ The surface composition in binary nanocrystalline compounds depends on faceting.^{18a} The surface of quasi-spherical PbS NCs has been found to be Pb-rich (Pb/S ~ 1.3 – 1.5),^{18b} and hence ~ 26 – $30 \text{ wt } \%$ of total sample weight will provide the stabilization of all undercoordinated Pb atoms at the surface with a 1 to 1 ratio. Note, that recently, a model of the stoichiometric PbSe core terminated by Pb atoms, two of those are coordinated by one molecule of oleic acid, has been proposed for PbSe NCs.^{18c} Based on the higher concentration of oleic acid in PFs, we assume a higher density of the capping molecules at the surface of PbS NCs in PFs as compared to DFs and CCs. Obviously, addition of alcohols during crystallization can strip off ligands from the surface of PbS NCs. Being more “diluted” at the surface of “washed” NCs, molecules of oleic acid should have a higher degree of freedom in terms of structural conformation.

The length of the fully extended molecule of oleic acid is $\sim 18 \text{ \AA}$. Prior to any thermal treatment, the center-to-center distance between closest neighboring NCs organized into the *fcc* lattice is $d = d_{111}\sqrt{6}/2 = 84 \text{ \AA}$ ($\pm 1 \text{ \AA}$). Based on the SAXS data, the size of inorganic core was found to be 70 \AA . It means that the interparticle spacing is 14 \AA that is significantly smaller than the length of a fully extended molecule of oleic acid. This observation allows us to exclude the full interdigitation of molecules from neighboring

NCs. Thus, organic molecules can either adopt other conformations than the fully extended one or still interdigitate at some cross points. In the case of PFs the interparticle spacing was found to be $\sim 18\text{--}19$ Å (by a pair distance function calculation, Figure S6, or by direct calculation from the position of d_{111} assuming perfect *fcc* symmetry, respectively) indicating an $\sim 25\%$ difference in the interparticle spacing between PFs and CCs. An interparticle spacing of 18 Å can allow the interdigitation of fully extended molecules. It is worth mentioning that the interparticle spacing is usually determined from transmission electron micrographs (TEM) acquired for 2D arrays of NCs. For instance, for PbS NCs, capped with oleic acid, the interparticle spacing estimated by TEM was found to be ~ 17 Å.⁵ It can be that, in close proximity to the substrate, organic molecules have different structures to maximize hydrophobic interactions with the substrate; however, this value does not necessarily coincide with the interparticle spacing in 3D structures.

Assuming that the "expanded state" of NC solids can better accommodate the possible structural transformation of the lattice, we kept PbS CCs at 180 °C for ~ 2 h. This led to the decrease of the center-to-center distance up to ~ 79 Å after the CCs were cooled down to room temperature. Since there is no change in the size of PbS NCs, this observation indicates that the interparticle spacing was decreased to ~ 9 Å. A similar trend in the interparticle spacing upon annealing at 150 °C, however, associated with an increase in disorder was reported for arrays of 6.2 nm PbSe NCs.¹⁹ In contrast, our SAXS data (Figure S7) taken from CCs before and after ~ 2 h of annealing at 180 °C demonstrated no change in the degree of ordering. HRSEM confirms that no sintering of individual NCs and no disordering took place during the annealing (Figure 1c,d). The total volume change of the effective size of CCs was $\sim 6\%$ (from 84 to 79 Å), while the interparticle spacing in annealed structures was modified by 36%. According to TGA data, no significant change in mass was observed for the sample heated at 180 °C for ~ 2 h (Figure S5). It means that change in the interparticle spacing can be associated with conformational or spatial changes of oleic acid. Thus, thermal treatment of NC solids can be considered as a promising approach allowing efficient control over particle separation. PFs and CCs have similar organization in terms of the crystalline lattice; however, they are quite different in terms of spacing between neighboring particles. In fact, to achieve values of the interparticle spacing equal to those found in CCs grown at room temperature, PFs need to be heated up to 260 °C, where individual NCs begin to undergo sintering. Annealing of the samples showed that all types of PbS NC solids were much more stable against sintering as compared to previously reported arrays of gold and silver NCs.^{13a} We believe that the thermal behavior of NC solids can significantly depend on the nature of the ligands used to stabilize the surface of the NCs. We expect that the proper choice of capping ligands in combination with thermal treatment is a promising route to control collective properties of 3D solids that can potentially lead to the miniband formation.²⁰ In spite of significant progress in the synthesis of NCs with controlled size, shape, and composition, there are only a few studies dedicated to the arrangement of capping ligands on the surface of individual NCs^{21a,b} and their impact on self-assembled structures.^{6a,21c} We hope our findings will stimulate studies directed toward understand-

ing the role of structure and structural deformation of organic molecules within NC solids during self-assembly and a postpreparative treatment.

Acknowledgment. The work is supported by the U.S. Department of Energy, Office of Science, Office of Basic Energy Sciences, under Contract No. DE-AC02-06CH11357. D.V.T. acknowledges financial support from the University of Chicago and NSF MRSEC Program under Award Number DMR-0213745.

Supporting Information Available: SAXS curves for the heat cycled samples (Figures S1–S4, S7); TGA data (Figure S5) and pair distance function (Figure S6) on DFs, PFs, and CCs (Figure S6). This material is available free of charge via the Internet at <http://pubs.acs.org>.

References

- (1) (a) Gur, I.; Fromer, N. A.; Geier, M. L.; Alivisatos, A. P. *Science* **2005**, *310*, 462–465. (b) Caruge, J. M.; Halpert, J. E.; Wood, V.; Bulović, V.; Bawendi, M. G. *Nat. Photon.* **2008**, *2*, 247–250. (c) Sun, S.; Murray, C. B.; Weller, D.; Folks, L.; Moser, A. *Science* **2000**, *287*, 1989–1992. (d) Talapin, D. V.; Murray, C. B. *Science* **2005**, *310*, 86–89.
- (2) Aleksandrovic, V.; Greshnykh, D.; Randjelovic, I.; Froemsdorf, A.; Kornowski, A.; Roth, S. V.; Klinke, C.; Weller, H. *ACS Nano* **2008**, *2*, 1123–1130.
- (3) (a) Murray, C. B.; Kagan, C. R.; Bawendi, M. G. *Annu. Rev. Mater. Sci.* **2000**, *30*, 545–610. (b) Murray, C. B.; Kagan, C. R.; Bawendi, M. G. *Science* **1995**, *270*, 1335–1338.
- (4) (a) Shevchenko, E.; Talapin, D.; Kornowski, A.; Wieckhorst, F.; Kötzler, J.; Haase, M.; Rogach, A.; Weller, H. *Adv. Mater.* **2002**, *14*, 287–290. (b) Talapin, D. V.; Shevchenko, E. V.; Kornowski, A.; Gaponik, N.; Haase, M.; Rogach, A. L.; Weller, H. *Adv. Mater.* **2001**, *13*, 1868–1871.
- (5) Shevchenko, E. V.; Talapin, D. V.; Murray, C. B.; O'Brien, S. *J. Am. Chem. Soc.* **2006**, *128*, 3620–3637.
- (6) (a) Henry, A.-I.; Courty, A.; Pileni, M.-P.; Albouy, P.-A.; Israelachvili, J. *Nano Lett.* **2008**, *8*, 2000–2005. (b) Talapin, D. V.; Shevchenko, E. V.; Murray, C. B.; Titov, A. V.; Kral, P. *Nano Lett.* **2007**, *7*, 1213–1219. (c) Whetten, R. L.; Shafiqullin, M. N.; Khoury, J. T.; Schaaff, T. G.; Vezmar, I.; Alvarez, M. M.; Wilkinson, A. *Acc. Chem. Res.* **1999**, *32*, 397–406.
- (7) Collier, C. P.; Saykally, R. J.; Shiang, J. J.; Henrichs, S. E.; Heath, J. R. *Science* **1997**, *277*, 1978–1981.
- (8) Su, K.-H.; Wei, Q.-H.; Zhang, X.; Mock, J. J.; Smith, D. R.; Schultz, S. *Nano Lett.* **2003**, *3*, 1087–1090.
- (9) (a) Bolhuis, P. G.; Frenkel, D.; Mau, S.-C.; Huse, D. A. *Nature* **1997**, *388*, 235–236. (b) Rudd, R. E.; Broughton, J. Q. *Phys. Rev. B* **1998**, *58*, 5893.
- (10) (a) Norris, D. J.; Arlinghaus, E. J.; Meng, L.; Heiny, R.; Scriven, L. E. *Adv. Mater.* **2004**, *16*, 1393–1399. (b) Hynninen, A.-P.; Dijkstra, M. *Phys. Rev. Lett.* **2005**, *94*, 138303.
- (11) Beverly, K. C.; Sample, J. L.; Sampaio, J. F.; Remacle, F.; Heath, J. R.; Levine, R. D. *Proc. Natl. Acad. Sci. U.S.A.* **2002**, *99*, 6456–6459.
- (12) Abécassis, B.; Testard, F.; Spalla, O.; Barboux, P. *Nano Lett.* **2007**, *7*, 1723–1727.
- (13) (a) Korgel, B. A.; Zaccheroni, N.; Fitzmaurice, D. *J. Am. Chem. Soc.* **1999**, *121*, 3533–3534. (b) Kiely, C. J.; Fink, J.; Brust, M.; Bethel, D.; Schiffrin, D. *J. Nature* **1998**, *396*, 444–446.
- (14) Hines, M. A.; Scholes, G. D. *Adv. Mater.* **2003**, *15*, 1844–1849.
- (15) van Huis, M. A.; Kunneman, L. T.; Overgaag, K.; Xu, Q.; Pandraud, G.; Zandbergen, H. W.; Vanmaekelbergh, D. *Nano Lett.* **2008**, *8*, 3959–3963.
- (16) Cai, Y.; Bernase, S. L. *J. Phys. Chem. B* **2005**, *109*, 4514–4519.
- (17) Lobo, A.; Möller, T.; Nagel, M.; Borchert, H.; Hickey, S. G.; Weller, H. *J. Phys. Chem. B* **2005**, *109*, 17422–17428.
- (18) (a) Cho, K. S.; Talapin, D. V.; Gaschler, W.; Murray, C. B. *J. Am. Chem. Soc.* **2005**, *127*, 7140–7147. (b) Cademartiri, L.; Bertolotti, J.; Sapienza, R.; Wiersma, D. S.; von Freymann, G.; Ozin, J. A. *J. Phys. Chem. B* **2006**, *110*, 671–673. (c) Moreels, I.; Fritzing, B.; Martins, J. C.; Hens, Z. *J. Am. Chem. Soc.* **2008**, *130*, 15081–15086.
- (19) Mentzel, T. S.; Porter, V. J.; Geyer, S.; MacLean, K.; Bawendi, M. G.; Kastner, M. A. *Phys. Rev. B* **2008**, *77*, 075316.
- (20) Lazarenkova, O. L.; Balandin, A. A. *J. Appl. Phys.* **2001**, *89*, 5509–5515.
- (21) (a) Jackson, A. M.; Myerson, J. W.; Stellacci, F. *Nat. Mater.* **2004**, *3*, 330–336. (b) Jackson, A. M.; Hu, Y.; Silva, P. J.; Stellacci, F. *J. Am. Chem. Soc.* **2006**, *128*, 11135–11149. (c) Hu, Y.; Uzun, O.; Dubois, C.; Stellacci, F. *J. Phys. Chem. C* **2008**, *112*, 6279–6284.

JA906632B